

## Unwinding globules under tension and polymer collapse

Thomas Frisch\* and Alberto Verga†

*Institut de Recherche sur les Phénomènes Hors Équilibre, 49, rue F. Joliot-Curie, Boîte Postale 146, 13384 Marseille, France*

(Received 16 July 2001; published 2 April 2002)

Polymer collapse is known to be mediated by the formation of pearls. These intermediate structures behave as small globules under tension. The globule size is studied by molecular dynamic simulations as a function of the strength of an external stretching force applied to its ends, for different values of the chain length. A very strong first-order-like transition from a compact globule state to a stretched one is observed. A model of this transition in terms of a globule-chain system is presented. The critical force, above which the globule unwinds, is shown to satisfy a power law scaling like  $N^{1/3}$  in the number of monomers.

DOI: 10.1103/PhysRevE.65.041801

PACS number(s): 61.41.+e, 87.15.Aa, 36.20.Ey

Proteins are synthesized as flexible polypeptides and they collapse into a specific compact form called the native form. The kinetics of the folding process is amazingly complex and an understanding of this folding process towards the native state is an important challenge [1–3]. In parallel, stretching experiments on single biomolecules [4] is now a rapidly developing field and may provide information on the elastic behavior of the molecules that take place during protein folding and give as well some insight into biological function. Even though single homopolymer chain are structurally simpler than proteins, the study of their elastic properties at equilibrium in a poor solvent [5–9], and the study of the dynamical behavior of the collapse from an extended shape to a compact globule during a rapid quench below the  $\Theta$  point [10–18], are active areas of research. Experimental investigations of the collapse or of the stretching of a homopolymer are sparse due to the enormous difficulty of following the folding of a single chain in a poor solvent at low concentration [19–22]. The picture that has now emerged, however, from these experimental and mainly from numerical studies is that the collapse process is mediated by the presence of small pearls (a cluster of monomers) linked to one another by a fluctuating stretched chain. Therefore, the full dynamics of the collapsing polymer is a complex process that depends, in particular, on the elastic response of each globule under tension, and on the quench history.

The problem of globule under a stretching force was previously addressed theoretically [5–9] and numerically [7,9]. These works showed that the behavior of a globule under the  $\Theta$  point share some similarities with a first-order transition. Below a critical stretching force the globule remains compact, and above the critical force the globule unwinds into a stretched chain. In this paper we investigate, theoretically and numerically, the mechanisms involved in this first-order-like transition, in order to clarify the origin of the critical force and their scaling properties with respect to the number of monomers. In the first part we describe the collapse from an extended shape to a compact globule using molecular dynamics in the canonical ensemble [23], and we discuss briefly the influence of the quench depth. In the second part,

we study a single pearl under tension at equilibrium, and we derive the force-extension relation.

We developed an efficient code to perform off lattice three dimensional molecular dynamics simulations of a homopolymer at finite temperature neglecting hydrodynamic effects. This approach allows us to study very long chains, and to follow their evolution using conservative dynamics in the canonical ensemble. In contrast to other methods there is no need to introduce arbitrary phenomenological parameters on which time scales will depend. We investigated, in particular, the collapsing transition of a  $N=3000$  polymer ( $N$  is the number of monomers), previous studies were conducted by different methods for smaller values of  $N$  (Monte-Carlo methods [13,14,17], Langevin methods [18]).

The numerical simulations were performed using the Nosé-Hoover method that permits us to work in the canonical ensemble (fixed temperature). The polymer chain contains  $N$  molecules interacting through a classical long-range van der Waals force. The connectivity of the chains is respected by using a strong anharmonic potential for neighboring monomers. The Nosé-Hoover equations for the monomer  $i$  are

$$\dot{\mathbf{r}}_i = \mathbf{p}_i / m_i, \quad (1)$$

$$\dot{\mathbf{p}}_i = - \frac{\partial V_i}{\partial \mathbf{r}_i} - \xi \mathbf{p}_i, \quad (2)$$

$$\tau_\xi^2 \dot{\xi} = \frac{2K}{k_B T} - (3N - 6). \quad (3)$$

Here  $\mathbf{r}_i$  and  $\mathbf{p}_i$  are the position and momentum,  $\xi$  is the “friction” variable,  $T$  the temperature ( $k_B$  the Boltzmann constant),  $\tau_\xi = 2Q/k_B T$  is the time constant of the heat bath ( $Q = \text{const}$ ), and  $K = \sum_{i=1}^N p_i^2 / 2m_i$  is the kinetic energy. The total number of degrees of freedom is  $3N - 6$  since we subtracted the translation and rotation of the center of mass. Overdots represent time derivatives. The potential  $V_i$  is the interaction energy of monomer  $i$  with all other monomers, it has two contributions  $V = V_1(r) + V_2(r)$  ( $r$  is the distance between monomers). (i) The valence interaction between two neighboring monomers  $V_1(r) = a(r - d_0)^2 + b(r - d_0)^4$ , where  $d_0$  is the equilibrium distance and  $a, b$  are constants

\*Electronic address: frisch@irphe.univ-mrs.fr

†Electronic address: verga@irphe.univ-mrs.fr

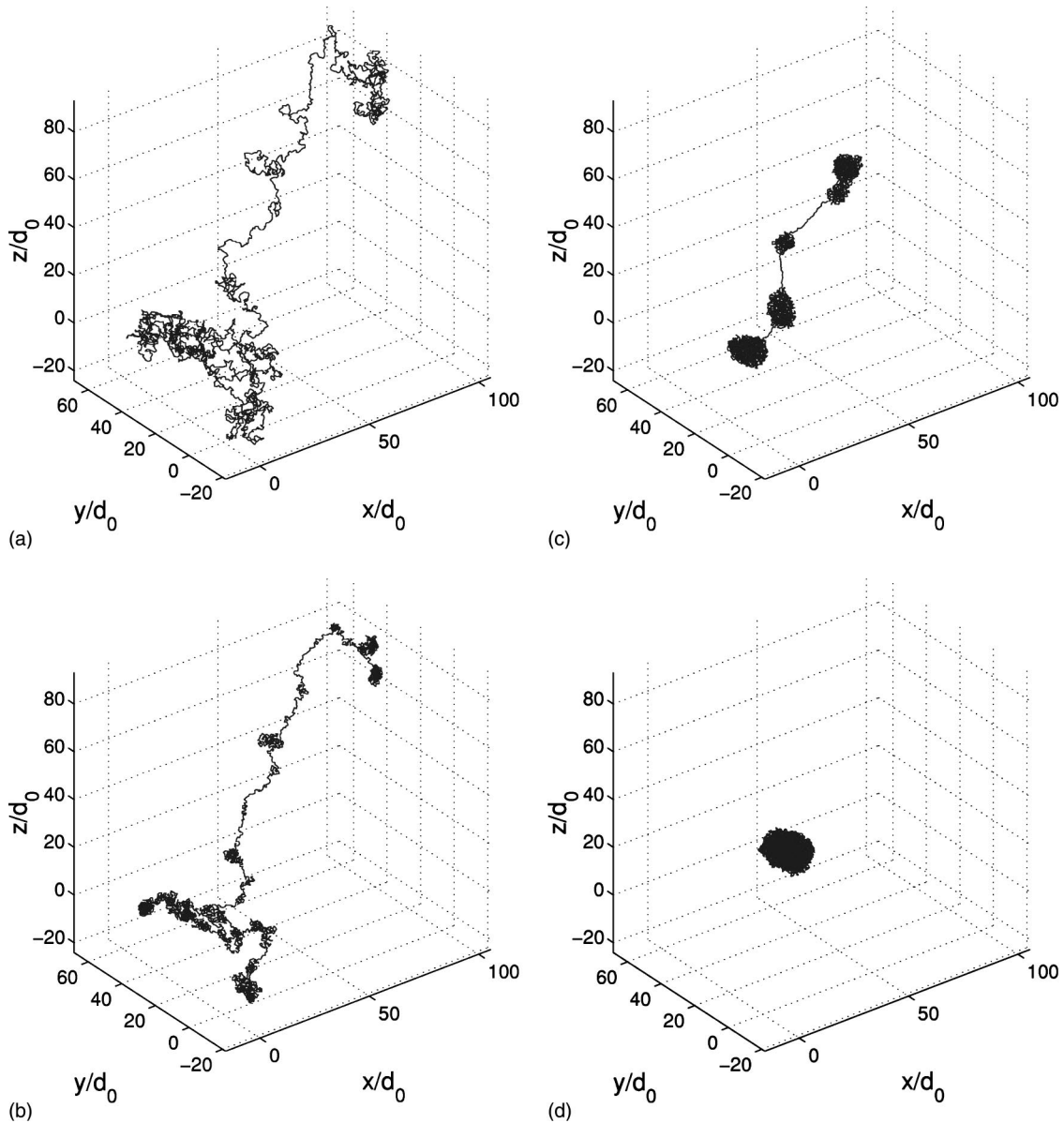


FIG. 1. Molecular dynamics simulation of a  $N=3000$  homopolymer. (a) A self-avoiding random walk generated by a Monte-Carlo method ( $t=0$ ). (b) Nucleation centers appear ( $t=3 \times 10^4 \Delta t$ ), this state is characterized by a set of pearls separated by stretched chains. (c) Merging of pearls accompanied by a shrinking of the polymer size ( $t=3 \times 10^5 \Delta t$ ). (d) Globular state ( $t=6 \times 10^5 \Delta t$ ).

characterizing the anharmonic interaction. (ii) The Lennard-Jones interaction between nonneighboring monomers,  $V_2(r) = \eta[(\sigma/r)^{12} - (\sigma/r)^6]$ , where  $\eta$  is the potential depth and  $\sigma$  the van der Waals radius. Molecular dynamic simulations were performed using an implicit Verlet-Newton-Raphson method for time stepping [23]. The parameters used are:  $d_0 = \sigma = 1.0$ ,  $\eta = 0.9$ ,  $a = 30$ ,  $b = 100$ ,  $Q = 10$ , the time step is  $\Delta t = 10^{-3}$ , and  $k_B T = 0.2$ . The  $\Theta$  point is about  $\Theta \approx 0.7$ , as obtained numerically for the chosen parameters. Units are based on  $d_0$  for lengths,  $k_B T$  for energies, and  $\Delta t$  for time.

In Fig. 1 we present the time evolution of a homopolymer ( $N=3000$ ) from an initial “swollen coil” state to the final (equilibrium) “globule” state. Similar results were obtained by another methods, Monte Carlo and Langevin simulations,

by different groups [13,14,17]. The initial state is a self-avoiding random walk modeling a polymer in a good solvent. The gyration radius  $R_g$  in the swollen coil state scales as  $N^{3/5}$ . At time  $t=0$  we quench the polymer below the  $\Theta$  point, in order to trigger the polymer collapse [Fig. 1(a)]. One can distinguish during the collapse different regimes: the initial “pearl formation” stage, the subsequent stretching of the linking chains accompanied by the pearl growth (“tension regime”), and finally, the pearl “coalescence regime,” which drives the polymer towards the globule state. Among these stages, the tension dominated regime is the longest one. We observe the creation of many pearls that start to grow by adsorbing monomers from the neighboring chains [Fig. 1(b)]. At this stage the total size of the polymer decreases slowly, showing that the clustering is essentially a local pro-

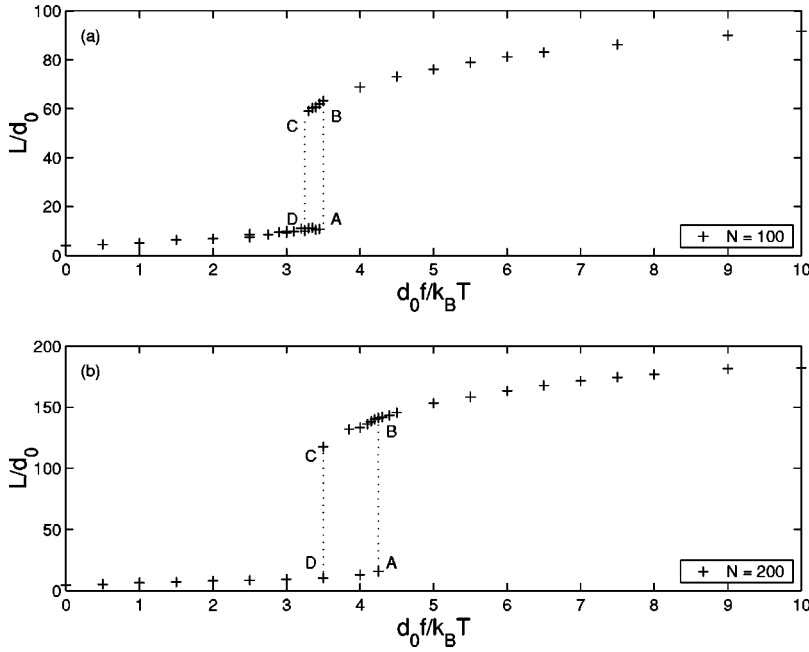


FIG. 2. End-to-end distance as a function of the tension  $L=L(f)$ . (a)  $N=100$ , (b)  $N=200$ . The points A, B, C, and D show the hysteresis cycle.

cess. The interaction between pearls is carried by the linking chains that stretch as pearls grow. Next, the pearls move towards each other and finally coalesce [Fig. 1(c)]. In this regime the strong tension created in the chains leads to a reduction of their thermal fluctuations. The final state consists of a compact globule with a gyration radius scaling as  $N^{1/3}$  [Fig. 1(d)]. Because of the existence of different regimes, each one having its own time scale, and a typical dependence on the thermodynamical variables  $N$  and  $T$  [12], one must rule out a simple description of the collapsing process. The different kinetic regimes with their characteristic time scales were extensively discussed in the literature [12,24]. These numerical results show that the collapse is largely dominated by the growth of pearls, their properties basically depend on the tension exerted by the neighboring chains. Moreover, each pearl evolves almost independently of others, as long as they are far apart. Therefore, it is interesting to study the behavior of a single pearl under tension, which constitutes a necessary step towards a full description of polymer collapse.

We have also studied the influence of the depth of the quench, here the temperature difference to the  $\Theta$  point. We found that as the quench depth increase, the pearls tends to transform into sausagelike objects, which were predicted theoretically by de Gennes [10]. A detailed account of this result will be published elsewhere, but the main effect can be explained in terms of the competition between the kinetic energy (slowing down of monomer mobility) and neighboring monomer attractive interactions.

In order to reproduce the behavior of a single pearl we use a short chain,  $N < 500$  typically, and we apply to its ends a constant tension  $f$ . We use as initial condition a well equilibrated globule [Fig. 1(d)]. The force applied to both ends is equal in magnitude and of opposite signs. We measure the mean end-to-end distance  $L$ , and the mean gyration radius  $R_g$  as a function of the force. The mean quantities are obtained by temporal averaging over large times at equilibrium. The

results of Fig. 2 show that two well defined states can be identified: a low tension state, for which the globule is only slightly deformed; and a high tension state for which the original pearl is stretched into a chain. Figure 3 shows the typical configuration of the polymer in the initial state, and below and above the critical force. As we increase the tension from zero the globule deforms elastically until a critical value  $f_A=f_B$  for which the globule is suddenly stretched out (Fig. 2). Above  $f_A$  the system, a stretched coil, is described by the near rod limit. When we decrease the tension, we observe that the length diminishes slowly, passes through the  $f_B$  point, and at  $f_C=f_D$  jumps back to the globule state. As  $f_C$  is smaller than  $f_A$  the transition between the two states is first-order-like and we have a hysteresis cycle.

Another quantity of interest is the gyration radius, which characterizes the globule size, and follows the same behavior as  $L$ . We observe [Figs. 3(a), 3(b), and 4] that the globule, in response to a small tension, slightly swells out. This elastic behavior results from the attractive interaction between monomers. It is dominated by internal energy and not by pure entropic effects. A simple theoretical explanation of this phenomenon is given by a model of a globule in equilibrium with a stretched chain [the globule-chain configuration of Fig. 3(b)]. The globule of  $N_g$  monomers is described by a free energy,

$$F_g = k_B T \left( -\frac{|B|N_g^2}{R^3} + \frac{CN_g^3}{R^6} \right), \quad (4)$$

where the entropic and surface terms were neglected,  $R$  is the globule size, it is related to the globule density  $n$ ,  $R \sim R_g \sim n^{-1/3}$ ;  $B=B(T)$  and  $C=C(T)$  are the second and third virial coefficients, respectively (up to a geometrical factor); below the  $\Theta$  temperature  $B < 0$  [25]. In the absence of

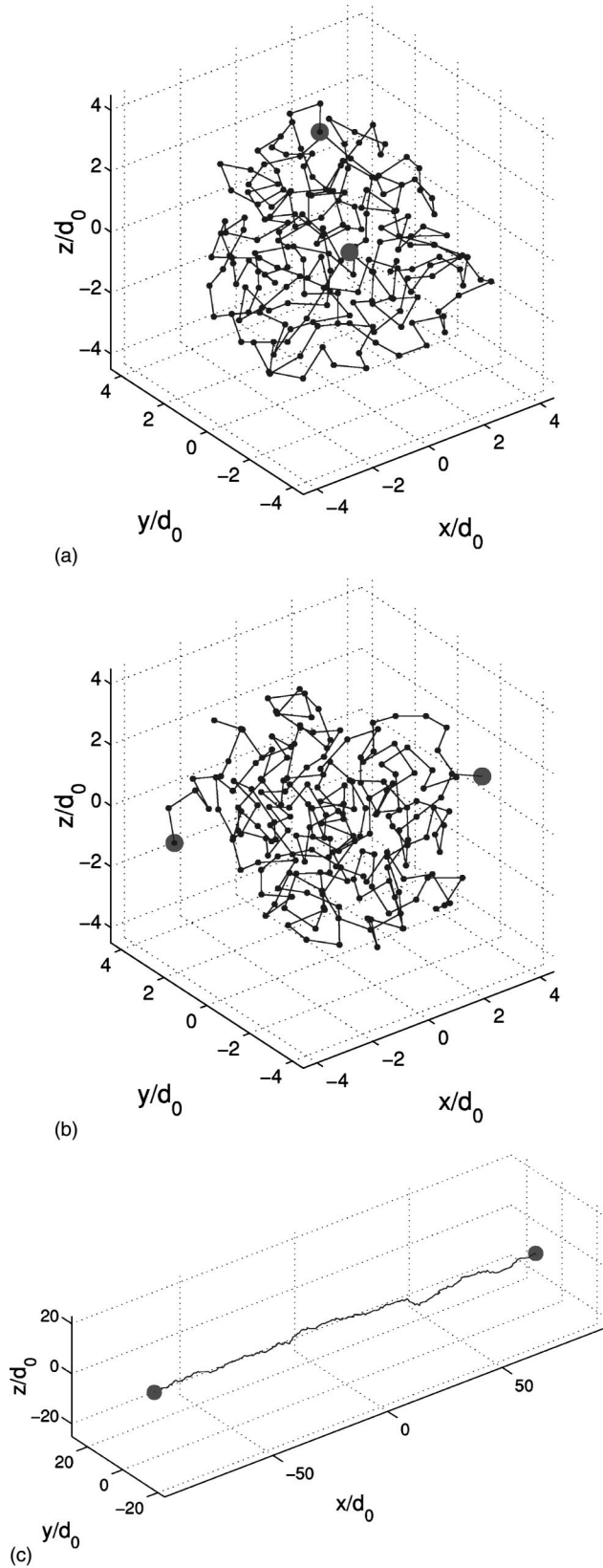


FIG. 3. Typical configurations of a  $N=200$  chain under tension. (a) the globule state for  $f=0$ , (b) the globule-chain state, below the transition  $d_0 f/k_B T=3.5$  ( $f < f_A$ ); and (c) the stretched chain state for  $d_0 f/k_B T=7.5$  ( $f > f_A$ ).

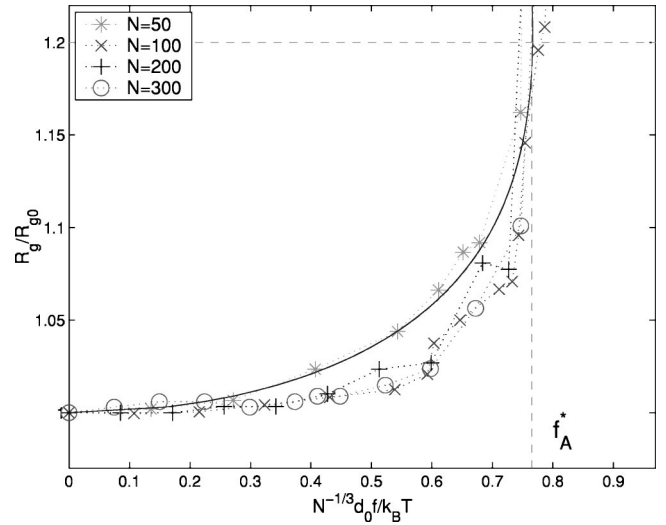


FIG. 4. Mean gyration radius  $R_g/R_{g0}$  as a function of the normalized tension  $N^{-1/3}f/k_B T$ , for various values of  $N$ . The solid line is the theoretical result from Eq. (6) (with  $\beta=1.7$ ); the horizontal dashed line represent the critical radius  $R_A/R_e=(7/4)^{1/3}$ , and the vertical one is the critical normalized force  $f_A^*$ .

tension the globule radius is simply given by  $R_e=(2CN_g/|B|)^{1/3}$ . The free energy of a freely joined chain under tension [the configuration of Fig. 3(c)] is given by the Langevin formula [25],

$$F_c = -k_B T N_c \ln \left( \frac{4\pi \sinh y}{y} \right), \quad y = \frac{d_0 f}{k_B T}, \quad (5)$$

where  $N_c$  is the number of monomers in the chain, and  $f$  the applied force; here  $F_c$  is an implicit function of the chain length  $R_c=N_c d_0(\coth y - 1/y)$ . When a force is applied to the globule an exchange of monomers with the chain is produced. The equilibrium state is established when the chemical potentials of the globule and the chain are identical. The chemical potential of the globule is  $\mu_g - \mu_{g0} = (\partial F_g / \partial R)(\partial R / \partial N_g)$ , where  $\mu_{g0} = (\partial F_g / \partial N_g)|_{R=R_e} = -k_B T B^2 / 4C$  is the chemical potential for  $f=0$ . Analogously, the chemical potential of the chain is  $\mu_c - \mu_{c0} = (\partial F_c / \partial R_c)(\partial R_c / \partial N_c)$ , where  $\mu_{c0} = (\partial F_c / \partial N_c)|_{f=0} = -k_B T \ln(4\pi)$ . From these two relations, and taking into account that  $dN_g = -dN_c$ , one obtains the equilibrium condition between the globule and the chain in the form  $(\partial F_g / \partial R) = -(\partial F_c / \partial R_c)|_{dR_c/dR}$ . As the tension is constant along the polymer, the globule density slightly diminishes, while the globule size  $R$  increases (see Figs. 3(b) and 4). As long as the number of monomers in the chain satisfies  $N_c \ll N_g \approx N$ , the chain-globule interactions are negligible, and one may assume that  $\Delta R$  and  $\Delta R_c$  are proportional:  $|dR_c/dR| \equiv 1/\alpha$ , where  $\alpha$  is independent of  $N_g$ . Moreover, in the regime of interest (globule-chain coexistence), the tension is large, so that  $y \gg 1$ . These conditions ensure that the globule-chain coupling is weak. From the equilibrium condition, and using that the chain length, for fixed  $N_c$ , is  $R_c = N_c d_0(\coth y - 1/y) \approx N_c d_0(1 - 1/y)$ , one obtains,

$$N^{-1/3} \frac{d_0 f}{k_B T} = \beta \left[ \left( \frac{R_e}{R} \right)^4 - \left( \frac{R_e}{R} \right)^7 \right]^{1/2}, \quad (6)$$

where  $\beta = (3\alpha d_0 |B| N^{4/3} / R_e^4)^{1/2}$ , is independent of  $N$  since  $R_e \sim N^{1/3}$ . To fit the numerical results with Eq. (6) we used  $\beta = 1.7$ . From this value of  $\beta$  one can compute the free parameter  $\alpha$ , which is found to be of order one  $\alpha = 0.4$  [26].

Equation (6) describes the elastic properties of the globule-chain system. Taking into account that the globule radius varies as  $R_e \sim N^{1/3}$ , the tension on the globule satisfies  $f \sim N^{1/3}$  in contrast to the  $N^{-1}$  behavior of the Gaussian coil. It is worth mentioning that this scaling law of the critical force with respect to the number of monomers was not obtained in previous works [5–9]. This may be due in part because most numerical studies dealt with the end-to-end distance, which is a highly fluctuating quantity.

We represented in Fig. 4 the graph of the  $R_g = R_g(f)$  function [normalized by  $R_{g0} = R_g(0)$ ], using the scaling suggested by Eq. (6) for various values of  $N$ . With the  $N^{1/3}$  scaling, the curves for different  $N$  appear to follow a single tendency. In particular, it is worth noting that the normalized critical force,  $f_A^* = N^{-1/3} d_0 f_A / k_B T$ , is the same for all  $N$ . The theoretical result (6) also predicts a critical force above which the globule cannot exist. At the critical point  $dR/df \sim \infty$  and the relation  $R_g = R_g(f)$  cannot be satisfied. A simple computation gives  $d_0 f_A(N) / k_B T = 0.45 \beta N^{1/3}$  for the critical force, and  $R_A / R_e = (7/4)^{1/3}$  for the corresponding radius of the globule. These theoretical results are in good agreement

with the numerical results obtained for  $N = 50$  to  $N = 300$ , in the region of validity of the approximations, near the critical force ( $y \gg 1$ ).

In conclusion, we have presented a theoretical model for the unwinding of a globule under tension and compared it with numerical simulations. The critical force, above which the globule unwinds, is shown to satisfy a power law  $N^{1/3}$  in the number of monomers. One immediate consequence of the elastic properties of globules is that two neighboring pearls separated by a well stretched chain, and having different sizes cannot be in equilibrium. The larger pearl exerts an attractive force on the smaller one, inducing a drift of the smaller pearl. Another effect, related to the critical force, is that during the initial stages of collapse, small pearls may easily unwind, if the local value of the tension is larger than the critical value. Furthermore, the process of pearl initial size selection, and the coalescence of small pearls into larger ones, may drive the system to a dynamical state characterized by a tension which is throughout near its own critical value.

It would be interesting to study experimentally the influence of the depth of the quench on the collapse. Another interesting issue would be to experimentally measure the force-extension relation, in order to detect the jump in the pearl size (end-to-end distance, gyration or hydrodynamic radius) in large biomolecules, polymers, DNA, or proteins, under appropriated conditions.

We acknowledge P. Marcq, J. Palmeri, and M. Abid for fruitful discussions.

- 
- [1] T.E. Creighton, *Protein Folding* (Freeman, New York, 1992).  
 [2] A. Fersht, *Structure and Mechanism in Protein Folding Science* (Freeman, New York, 1999).  
 [3] H. Frauenfelder, P.G. Wolynes, and R.H. Austin, *Rev. Mod. Phys.* **71**, S419 (1999).  
 [4] T. Strick, J. Allemand, D. Bensimon, and V. Croquette, *Annu. Rev. Biophys. Biomol. Struct.* **29**, 523 (2000).  
 [5] A. Halperin and E.B. Zhulina, *Macromolecules* **24**, 5393 (1991).  
 [6] A. Halperin and E.B. Zhulina, *Europhys. Lett.* **15**, 417 (1991).  
 [7] M. Wittkop, S. Kreitmeier, and D. Göritz, *Phys. Rev. E* **53**, 838 (1996).  
 [8] P.Y. Lai, *Phys. Rev. E* **53**, 3819 (1996).  
 [9] R.G. Maurice and C.C. Matthai, *Phys. Rev. E* **60**, 3165 (1999).  
 [10] P.G. de Gennes, *J. Phys. (France) Lett.* **46**, L639 (1985).  
 [11] A. Buguin, F. Brochard-Wyart, and P.G. de Gennes, *C. R. Acad. Sci. Paris, Série 2* **322**, 741 (1996).  
 [12] A. Halperin and P.M. Goldbart, *Phys. Rev. E* **61**, 565 (2000).  
 [13] B. Ostrovsky and Y. Bar-Yam, *Europhys. Lett.* **25**, 409 (1994).  
 [14] B. Ostrovsky and Y. Bar-Yam, *Biophys. J.* **48**, 1694 (1995).  
 [15] A. Pitard and H. Orland, *Europhys. Lett.* **41**, 467 (1998).  
 [16] E. Pitard and J.P. Bouchaud, *Eur. Phys. J. E* **5**, 133 (2001).  
 [17] Y.A. Kuznetsov, E.G. Timoshenko, and K.A. Dawson, *J. Chem. Phys.* **103**, 4807 (1995).  
 [18] A. Byrne, P. Kiernan, D. Green, and K.A. Dawson, *J. Chem. Phys.* **1**, 573 (1995).  
 [19] B. Chu, Q. Ying, and A.Y. Grosberg, *Macromolecules* **28**, 180 (1995).  
 [20] C. Wu and S. Zhou, *Phys. Rev. Lett.* **77**, 3053 (1996).  
 [21] M. Nakata and T. Nakagawa, *Phys. Rev. E* **56**, 3338 (1997).  
 [22] B. Haupt, T. Senden, and E. Sevick, *Experimental Evidence of the Rayleigh Instability in Single Polymer Chains* (APS, Seattle, 2001), <http://www.aps.org/meet/MAR01/baps/abs/G2690009.html>.  
 [23] D. Frenkel and B. Smit, *Understanding Molecular Simulations* (Academic Press, New York, 1996).  
 [24] E.G. Timoshenko, Y.A. Kuznetsov, and K.A. Dawson, *J. Chem. Phys.* **104**, 3338 (1996).  
 [25] A.Y. Grosberg and A.R. Khokhlov, *Statistical Physics of Macromolecules* (AIP Press, New York, 1994).  
 [26] The virial coefficient is estimated using the definition  $B = (3/2) \int [1 - \exp(-V_2/k_B T)] r^2 dr \approx 1.5$ , for  $\eta = 0.9$  and  $k_B T = 0.2$ .